National Conference with International Participation

ENGINEERING MECHANICS 2008

Svratka, Czech Republic, May 12 – 15, 2008

ANALYSIS OF CONTACT OF SURFACES USING THEORY OF SCREWS

J. Švígler[*] V. Machulda[**]

Summary: *This contribution deals with the analysis of three member mechanical system with higher kinematical pair which is created by conjugated screw surfaces. Axes of both surfaces, which are loaded by a force system, are in a skew position. The analysis of the local incorrect contact of conjugated screw surfaces with respect to influence of the force contact character is made by using the theory of screws. Difference between the normal force acting in the isolated contact point and in the point of the contact curve is shown.*

1. Introduction

Bodies of three member mechanic systems with higher kinematical pair have their contact at a point or curve. In consequence of force and temperature strain the position of bodies is changed and therefore a modification of character of the contact take place. In this paper the higher kinematical pair, that is created by two screw surfaces with parallel axes, have in the theoretical position the correct contact at the curve. In consequence of a machine inaccuracy and the force and temperature loading the originally parallel position of axes changes into a skew position. This change causes the variation of the surface contact character and their relative motion. The curve contact changes into contact at the point and the originally relative rolling motion changes into a spatial motion. Instantaneous state of the relative motion of both surfaces is possible to express with a force screw, wrench, and kinematical screw, twist. This contribution deals with the analysis of the local incorrect contact of conjugated screw surfaces with using of the theory of screws with the view to influence the force contact character. An aim of this paper is to determine the force, acting between both conjugated surfaces at the contact point in instantaneous time. Magnitude of the normal force, that is determined by force field rising outside surfaces and acting on each of them, depends on a form these surfaces and can be influenced by their shape. This quantity is important for a determination of a local surface strain. Used theory of screws is applied to screw machines i.e. screw compressors and screw engines which are generated by combination of compressors and expanders. Screw machines contain toothed rotors with complicated and specified screw surfaces.

[*] Doc. Ing. Jaromír Švígler, CSc.: Department of Mechanics, University of West bohemia; 306 14 Pilsen; tel.: +420 377 632 324, fax: +420 377 632 302; e-mail: svigler@kme.zcu.cz

[**] Ing. Vladimír Machulda: Department of Mechanics, University of West bohemia; 306 14 Pilsen; tel.: +420 377 632 382, fax: +420 377 632 302; e-mail: machulda@kme.zcu.cz

2. Kinematical screws, twists

Let us consider two rigid bodies 2 and 3 with a spatial moving. Kinematical state each of them is determined with instantaneous twist $\eta_3 : \omega_3, p_3,\quad \eta_2 : \omega_2, p_2$ around skew axes o_2, o_3, Fig. 1. where p_i, $i = 2, 3$ marks parameter of twist. Relative motion both bodies is given by relative twist $\eta_{32} : \omega_{32}, p_{32}$ around an axis o_{32} which position is determined by the mutual position of axes o_2, o_3 that is given by their shortest distance, transversal, a and the angle $\Sigma = \gamma_2 + \gamma_3$.

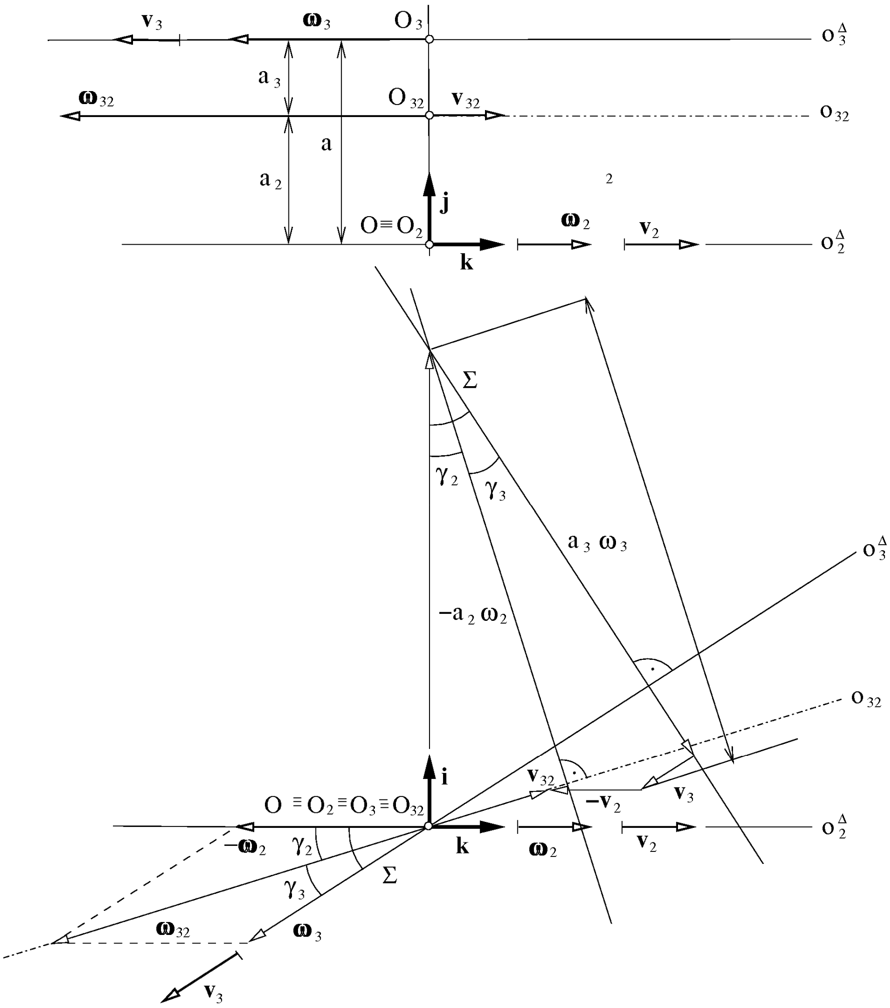

Fig. 1: Configuration of twist axes

Then the position of the axis of relative twist o_{32} can be determined (Šejvl, 1967, Švígler et al., 2006) in an auxiliary coordinate system $R_2 \equiv (\mathbf{i}_2, \mathbf{j}_2, \mathbf{k}_2)$ with the transversal a_2 and angle γ_2

$$a_2 = \frac{\sin\gamma_2}{\sin\Sigma}[a\cos\gamma_3 + (p_3 - p_2)\sin\gamma_3] \ ,$$

$$tg\gamma_2 = \frac{\sin\Sigma}{\dfrac{1}{i_{32}} + \cos\Sigma} \ . \qquad (1)$$

Both quantities we get from system of equations, Fig. 1,

$$a = a_2 + a_3 \ , \quad \Sigma = \gamma_2 + \gamma_3 \ ,$$

$$\omega_2 \sin\gamma_2 = \omega_3 \sin\gamma_3 \, , \quad \omega_3 = i_{32}\, \omega_2 \ , \tag{2}$$

$$a_2\, \omega_2 \sin\gamma_2 + v_2 \sin\gamma_2 = a_3\, \omega_3 \sin\gamma_3 + v_3 \sin\gamma_3 \ ,$$

that can be obtained using of classical kinematical way. Kinematical quantities ω_{32}, v_{32} of the relative twist are given, Fig. 1, with expressions

$$\omega_{32} = \omega_3 \sin\gamma_3 + \omega_2 \cos\gamma_2 \ ,$$

$$v_{32} = a_2\, \omega_2 \sin\gamma_2 + a_3\, \omega_3 \sin\gamma_3 - v_2 \cos\gamma_2 - v_3 \cos\gamma_3 \tag{3}$$

and the parameter of the twist is

$$p_{32} = \frac{v_{32}}{\omega_{32}} = \frac{\sin\gamma_2 \sin\gamma_3}{\sin\Sigma}\left(a - \frac{p_3}{tg\gamma_3} - \frac{p_2}{tg\gamma_2} \right) . \tag{4}$$

The axis o_{32} creates a line of a skew straight line surface of the 3rd degree, Plücker conoid, Fig. 2. This surface, that is a locus of twists resulting from composition of twists with varying ratio on two given skew straight line can be determined (Kadeřávek at al., 1932) by elliptical section k of circular cylindrical surface, straight line d and a vanishing line of the first plane of projection, π, Fig. 3. This surface has two torsal planes τ_1, τ_2 and each of which contains one torsal line t. These

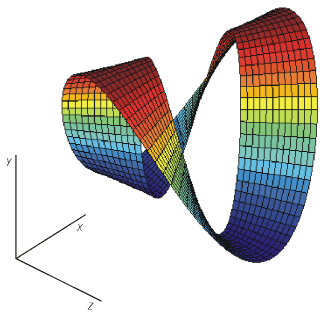

Fig. 2: Plücker conoid

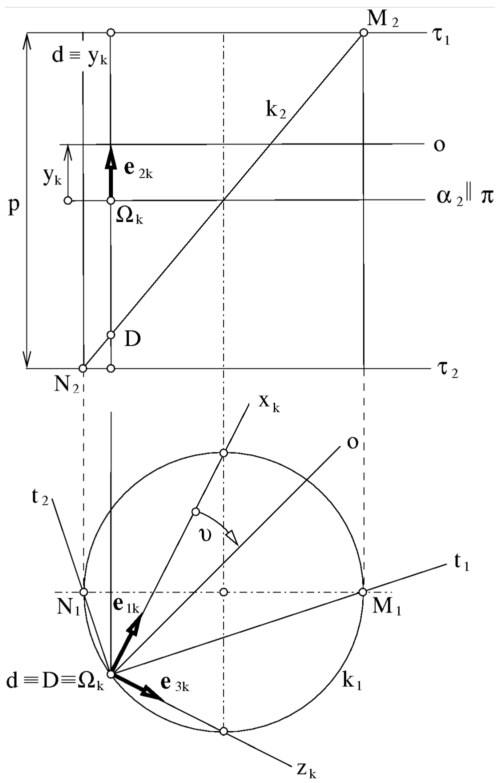

Fig. 3: Basic geometry of the Plücker conoid

torsal lines t_1, t_2 are perpendicular each other. There are further two intersecting straight line on the Plücker conoid which are perpendicular each other too. Their point of intersection Ω_k lies at a half of the conoid height p. These straight lines are called principal lines of the Plücker conoid and together with the straight line d create the fundamental coordinate system of the Plücker conoid $R_k = (\mathbf{e}_{1k}\, , \mathbf{e}_{2k}\, , \mathbf{e}_{3k})$. In the fundamental coordinate system of the Plücker conoid some line o some line o of this surface can be expressed

$$y_k = p \sin\vartheta \cos\vartheta \ , \qquad z_k = x_k\, tg\vartheta \ , \tag{5}$$

where p is a distance between two torsal planes and ϑ is an angle which the line o contains with the axis x_k. Geometric and kinematics connections between twists $\eta_2, \eta_3, \eta_{32}$, lying on lines o_2, o_3, o_{32}, can be demonstrated, Fig. 4, with using of the Disteli circle. From this circle the position of the axis o_{32} and the parameter p_{32} of the relative twist η_{32} can be determined. In a special case, given by relation $p_2 = p_3 = 0$, twists $\eta_3 : \omega_3, p_3$ and $\eta_2 : \omega_2, p_2$, transform into rotary motion, the abscissa $\overline{MN}$ fuses with $\overline{AB}$ and the point C transfers into the point H, so $p_{32} = 0$. The axis o_{32} creates bewelled skew ruled surfaces by rotary motion around axes o_2, o_3 conse cutively which take contact at the axis o_{32}.

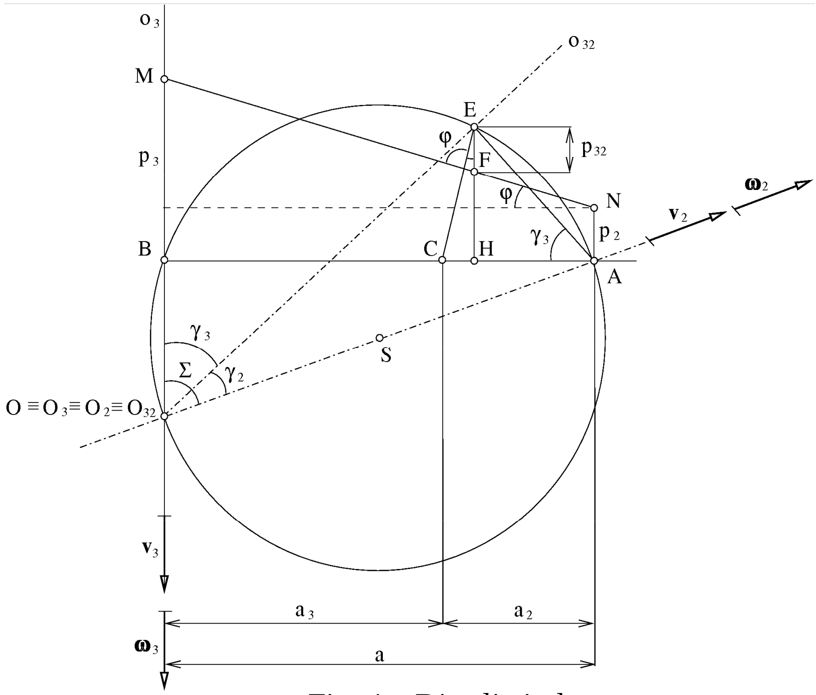

Fig. 4: Disteli circle

These surfaces create axodes of the relative twist. In a case that twists η_2 and η_3 change into rotary motion with angular velocities ω_2, ω_3 the bewelled skew ruled surfaces transform into surfaces of rotary hyperboloids of one sheet. Skew ruled surfaces are determined by their parameter distribution which can be determined from the equation system (2). From kinematical point of view the skew ruled surface is created by a motion of the straight line o_{32} that is caused by components of vectors $\mathbf{v}_2, \boldsymbol{\omega}_2, \mathbf{v}_3, \boldsymbol{\omega}_3$ which are perpendicular to the axis o_{32}. The parameter distribution of this skew ruled surface is expressed then as a ration of the velocity of the translational motion and the angular velocity. The parameter distribution of axodes of the relative twist (Šejvl, 1967) is possible to expressed with form

$$\delta = \frac{\cos\gamma_2 \cos\gamma_3}{\sin\Sigma}\left(a + p_3\, tg\,\gamma_3 + p_2\, tg\,\gamma_2\right) . \qquad (6)$$

The parameter distribution, that is the same for both axodes, can be illustrated, Fig. 4, with the abscissa EF'. Generating of the Plücker conoid is demonstrated in Fig. 5. General stright line is determined in the fundamental coordinate system R_k with Eq. (5). This coordinate system can be determined by using of the kinematics in the following way. Let us consider, Fig. 6, two screws $\Theta_\alpha : \omega_\alpha, p_\alpha$, $\Theta_\beta : \omega_\beta, p_\beta$, perpendicular each other, that lie upon the principal straight lines o_α, o_β of the Plücker conoid. By composition of these screws we obtain the screw $\Theta : \omega_\Theta, p_\Theta$, lying on the Plücker conoid which is determined with

$$p_\Theta = p_\alpha \cos^2\vartheta + p_\beta \sin^2\vartheta \ , \qquad y_\Theta = \left(p_\alpha - p_\beta\right)\sin\vartheta\cos\vartheta \ . \qquad (7)$$

Let be remarked that it is identical if we discussed about the twist or wrench. Now we consider a reciprocal problem. For two given screws $\Theta_2(\omega_2,\ p_2)$ and $\Theta_3(\omega_3,\ p_3)$ we want to determine principal screws $\Theta_\alpha, \Theta_\beta$. Applying of the equation (7) to each screw Θ_2, Θ_3, using relations $\Sigma = \vartheta_2 + \vartheta_3$ and $a = y_3 - y_2$, we obtain, after ordering, followed relations

$$p_\alpha - p_\beta = \frac{\sqrt{a^2 + (p_3 - p_2)}}{\sin\Sigma} \ ,$$

$$p_\alpha + p_\beta = p_3 + p_2 - a\cot g\,\Sigma \ ,$$

$$v_3 = \frac{1}{2}\left(\Sigma + arctg\,\frac{p_3 - p_2}{a}\right), \quad (8)$$

$$y_3 = \frac{1}{2}[(p_2 - p_3)\cot g\,\Sigma + a] \ ,$$

which determine the principal screws $\Theta_\alpha, \Theta_\beta$ appertaining to screws Θ_2, Θ_3.

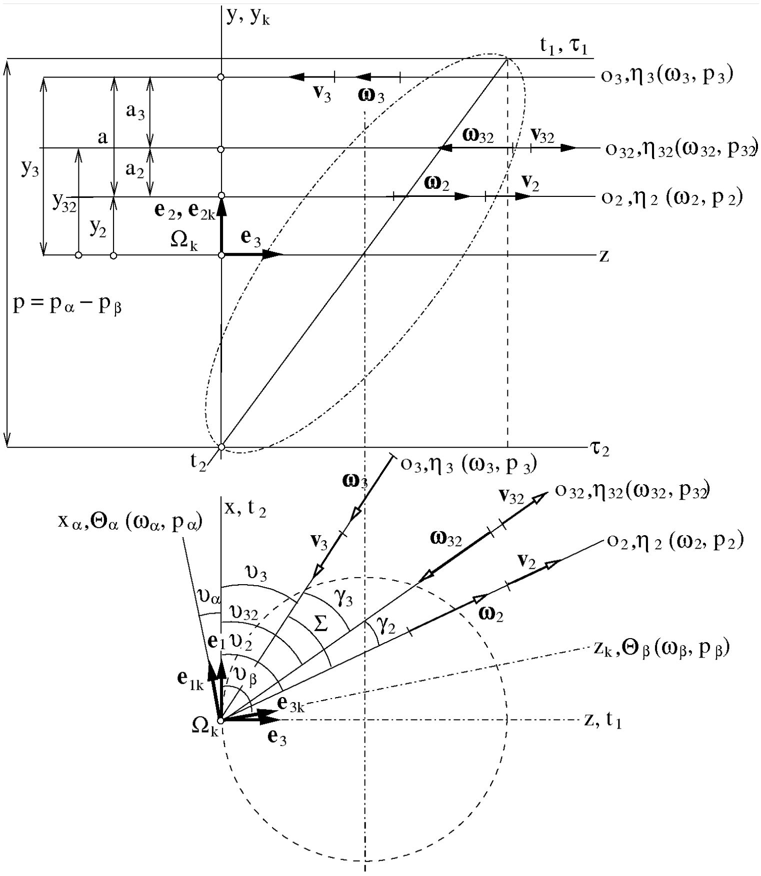

Fig. 5: Generating of the Plücker conoid

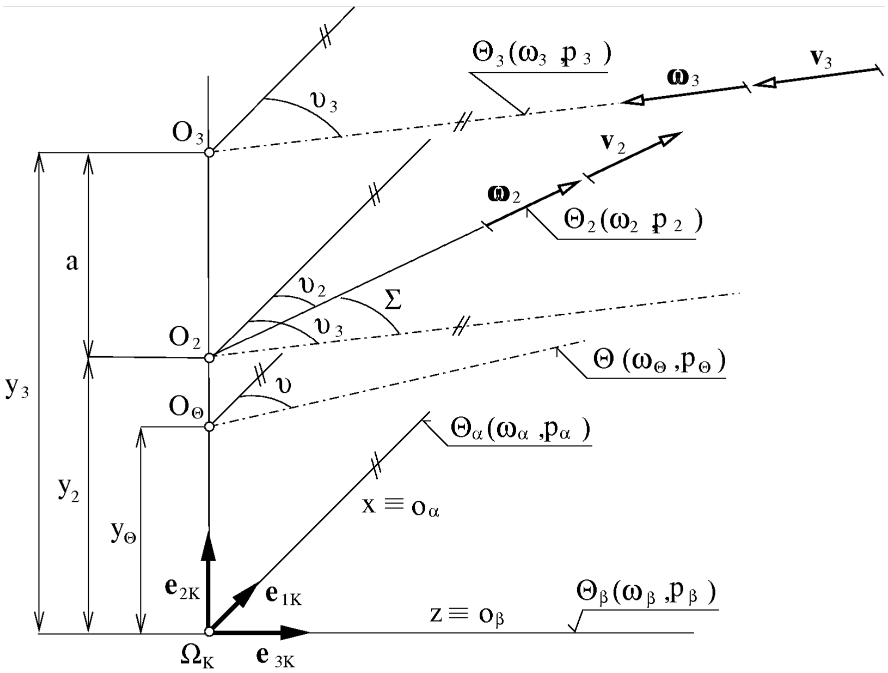

Fig. 6: Principal lines o_α, o_β and general line of the Plücker conoid

3. Force screw, wrench

As was said the equation (5) and equations (7), (8) are valid both twists and wrenches. Let us now consider a rigid body loaded by force field that is caused by medium pressure on the surface of the body. The result of this pressure is a rise of an instantaneous force field. The force field which consist from forces and couples in nodes L_k of selected coordinate axis, Fig. 7 was determined with relations

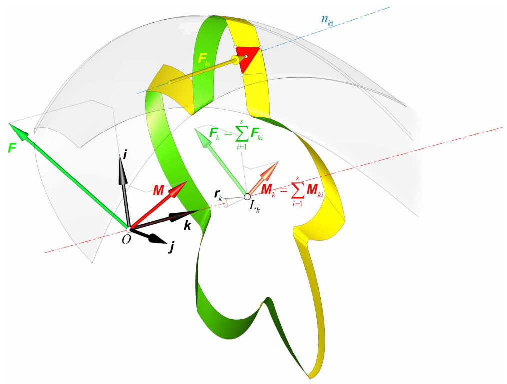

Fig. 7: Force effects on surface element

$$\mathbf{F}_k = \sum_{i=1}^{s} \mathbf{F}_i \ , \quad \mathbf{M}_k = \sum_{i=1}^{s} \mathbf{M}_i \tag{9}$$

where $\mathbf{F}_i$, $\mathbf{M}_i$ are results of the pressure on an elementary area of surface transformed into node k, $k = 1 \div n$, of the axis. Resultant of the force field is given with expressions

$$\mathbf{F} = \sum_{k=1}^{n} \mathbf{F}_k \ , \quad \mathbf{M} = \sum_{k=1}^{s} \mathbf{M}_k + \sum_{k=1}^{s} \mathbf{r}_k \times \mathbf{F}_k \ . \tag{10}$$

Both resultants **F, M** can be replaced with wrench that is determined by direction of forces and a position vector $\mathbf{r}_E = \mathbf{F} \times \mathbf{M} / |\mathbf{F}|$. Let us suppose a body performing a spatial motion which is given by the twist $\eta : \eta', \, p_\eta$ where η denotes kinematical screw η with the axis η, amplitude of the twist η' and the pitch of the screw p_η. The body is loaded by force field represented by the wrench $\rho : \rho'', \, p_\rho$ where ρ denotes force screw ρ with the axis ρ, intensity of the wrench, force, ρ'' and the pitch of the screw p_ρ. Then the instantaneous virtual work (Ball, 1998) done by the given twist against the given wrench is

$$W = 2\rho''\eta'\tilde{\omega}_{\rho\eta} = \rho''\eta' \left[(p_\rho + p_\eta)\cos\phi - d\sin\phi \right] , \tag{11}$$

where $\tilde{\omega}_{\rho\eta} = \frac{1}{2}\left[(p_\rho + p_\eta)\cos\phi - d\sin\phi \right]$ is the virtual coefficient in which d is the shortest distance between ρ , η and ϕ is the angle between ρ and η. Using the equation (11) the wrench ρ can be replaced with six wrenches $\rho_i : \rho_i'', \, p_{\rho_i}$, $i = 1 \div 6$, in six given screw axes ρ_i. Let us consider six arbitrarily twists η_j, $i = 1 \div 6$, appertaining to the body. The six wrenches ρ_i can be obtained under the condition that virtual work of the wrench ρ, acting against one of the six arbitrarily selected twist η_j, must do the same quantity of work as the sum of the six wrenches ρ_i acting against the same twist η_j. By taking five other twist η_j five more equations for ρ_i are obtained. It stands to reason that after replacing wrenches ρ_i with reciprocal wrenches ρ_i^R the sum of virtual work which was done by the wrench ρ and the reciprocal wrenches ρ_i^R must be zero. Then it is possible to speak about equilibrium of wrenches ρ and ρ_i^R where ρ_i^R are wrenches expressing reaction force effects. Let be noticed that the determination of six screw ρ_i, or ρ_i^R, on arbitrarily chosen axes ρ_i, denotes the determination of six intensities ρ_i'' or $\rho_i''^R$ laying on these axes. Hence pitches of these wrenches ρ_i, or ρ_i^R, and the wrench ρ must be the same. Then we obtain a classical case of the spatial problem in that the space force system, represented with wrench ρ, and reaction forces $\rho_i''^R$ on six given axes take a equilibrium.

4. Application

Application is focused in screw machines, i.e. screw compressors and engines, with liquid injection in which tooth surfaces of rotors beside of creation of a workspace and its sealing ensure the kinematical and force accouplement both rotors. The force field, caused by compression of medium in chambers of the screw machine, is considered in the phase just before the opening of the discharge which is given by angle of roll of the male rotor $\varphi_3 = 0^\circ$. Numerical solution was made for following geometric parameters of the screw machine: axes distance $a_w = 85\,mm$, gear ration $i_{32} = 1,2$, where 2 marks the female rotor and 3 is the male rotor, helix angle on the rolling cylinders of both rotors $\gamma = 45^\circ$, length of tooth parts of rotors $l = 193{,}8$ mm. Resultants of the force field, acting to each of both rotors, are given with eq. (10), Both resultants $\mathbf{F}_i, \mathbf{M}_i$, $i = 2, 3$, Fig. 8, can be replaced with wrenches $\rho_i : \rho_i''$,

$p_{\rho_i} \wedge \rho_i'' = F_i$, $\quad \rho_i'' p_{\rho_i} = M_{O_i}$, $i = 2, 3$. According classical mechanic action and reaction effects take the equilibrium which is expressed with

$$\mathbf{F}_i + \mathbf{R}_{A_i} + \mathbf{R}_{B_i} = \mathbf{0} \ ,$$

$$\left(\mathbf{r}_{B_i} - \mathbf{r}_{A_i}\right) \times \mathbf{R}_{B_i} - \mathbf{r}_{A_i} \times \mathbf{F}_i + \mathbf{M}_i + \mathbf{M}_{S_i} = \mathbf{0} \ , \tag{12}$$

$i = 2, 3$ where $\mathbf{M}_{S_i}$ are thought couple of forces lying on axes o_i added to rotors for the equilibrium. It was necessary to use this couple of forces then conjugated screw tooth surfaces of meshing rotors touch each other in a curve and distribution of normal forces along this curve is unknown. Results of the numerical solution the equation (15) under the mentioned condition for the angle of role $\varphi_3 = 0^\circ$ of the male role are presented in Tab. 1.

Tab. 1: Components of wrenches, reaction forces and their location for $\varphi_3 = 0^\circ$

Wrenches						
	Male rotor			Female rotor		
components	$\mathbf{F}_3\,[N]$	$\mathbf{M}_{o3}\,[Nm]$	$\mathbf{r}_{E_3}\,[m]$	$\mathbf{F}_2\,[N]$	$\mathbf{M}_{o2}\,[Nm]$	$\mathbf{r}_{E_3}\,[m]$
x	2048.51	-22.85	0.023	2287.26	-6.27	0.009
y	-2386.28	26.62	-0.044	2407.82	-6.60	0.012
z	-1251.39	13.96	0.122	-313.54	0.86	0.153

Reaction forces				
components	$R_{A_3}\,[N]$	$R_{B_3}\,[N]$	$R_{A_2}\,[N]$	$R_{B_2}\,[N]$
x	670.96	1377.55	821.17	1466.09
y	-901.69	-1484.59	812.40	1595.42
z	0.00	-1251.39	0.00	-313,54

In consequence of the accepted condition obtained results are not exact but they are sufficient for further solution.

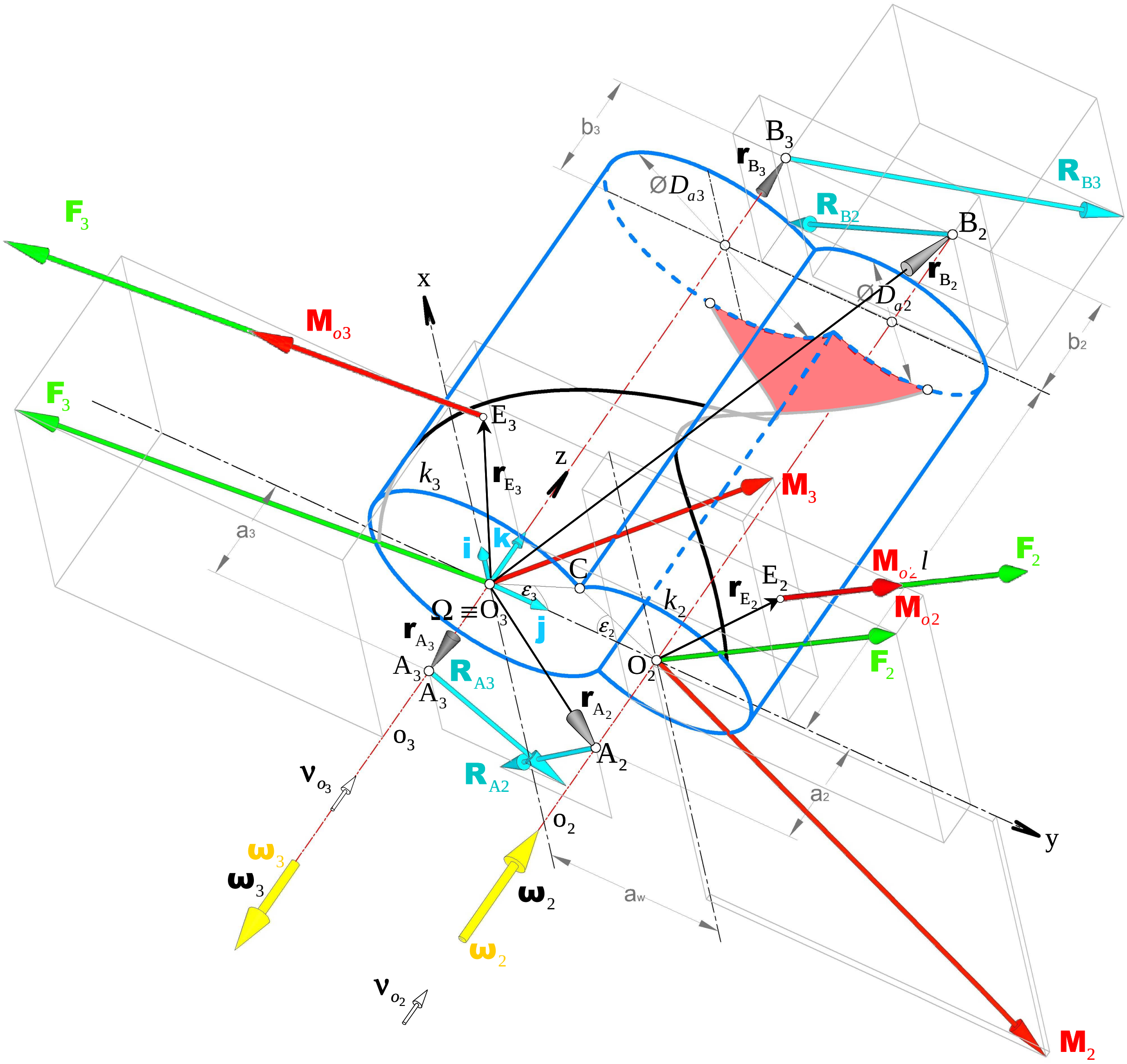

Fig. 8: Wrenches and reaction forces at seating of rotors

Except the force field the screw machine housing is loaded by a temperature field. Distribution of the temperature field acting to housing, which was obtained by measurement, is presented in Fig. 9. Displacements of bearing centers $\mu_{A_i}, \mu_{B_i}, i = 2, 3$, caused by force and temperature fields is presented in Tab. 2. Displacements of bearing centers are demonstrated in Fig. 10. A coordinate system $R \equiv (\mathbf{i}, \mathbf{j}, \mathbf{k})$, in which the undeformed position of the male rotor axis o_3 coalesces with coordinate axis z, creates the basic coordinate system. The position of rotors in the basic coordinate system R is determined with relations $\mathbf{r}_{O_3} = [0, 0, 0]^T$, $\mathbf{r}_{O_2} = [0, a_w, 0]^T$ and $\mathbf{v}_{O_3} = \mathbf{v}_{O_2} = [0, 0, 1]^T$.

After a bearing displacements axes o_3, o_2 translate into new positions $o_2^{\Delta}, o_3^{\Delta}$ which are determined with position vectors $\mathbf{r}_{o_3^{\Delta}} = \lfloor \Delta x_{o_3^{\Delta}}, \Delta y_{o_3^{\Delta}}, \Delta z_{o_3^{\Delta}} \rfloor^T$, $\mathbf{r}_{o_2^{\Delta}} = \lfloor \Delta x_{o_2^{\Delta}}, \Delta y_{o_2^{\Delta}}, \Delta z_{o_2^{\Delta}} \rfloor^T$ and unit vectors $\mathbf{v}_{O_3^\Delta} = \left[\cos\lambda_x^3, \cos\lambda_y^3, \cos\lambda_z^3, \right]^T$, $\mathbf{v}_{O_2^\Delta} = \left[\cos\lambda_x^2, \cos\lambda_y^2, \cos\lambda_z^2, \right]^T$. Relative position of axes o_2^Δ, o_3^Δ is given by the transversal $\mathbf{d}$ and angle Σ^Δ which are defined with relations

$$\mathbf{r}_{o_3^\Delta} + \mathbf{r}_{D_3} + \mathbf{d} + \mathbf{r}_{D_2} = \mathbf{r}_{o_2^\Delta} \ , \qquad \cos\Sigma^\Delta = \frac{\mathbf{v}_{o_3^\Delta} \cdot \mathbf{v}_{o_2^\Delta}}{\left|\mathbf{v}_{o_3^\Delta}\right| \cdot \left|\mathbf{v}_{o_2^\Delta}\right|} \ . \qquad (13)$$

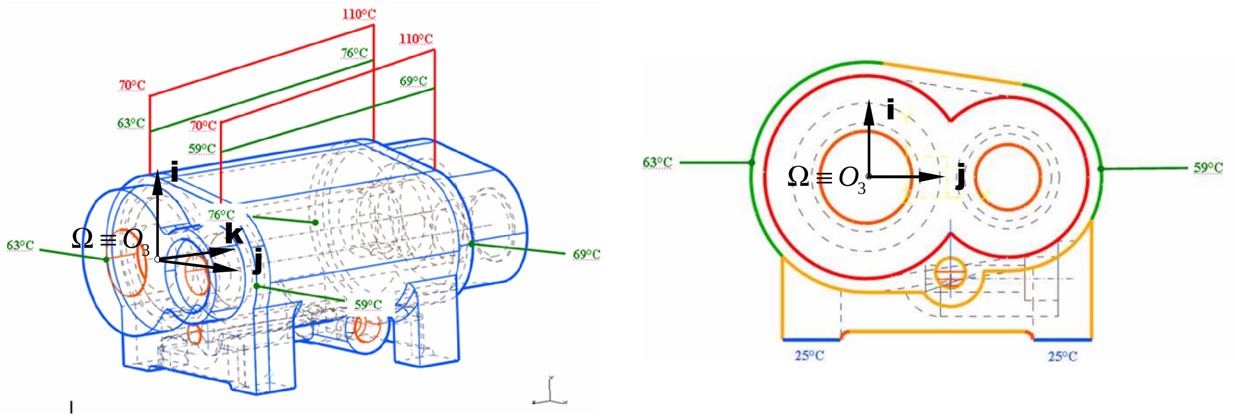

Fig. 9: Temperature field

Tab. 2: Displacements of bearing centers

Components	$\mathbf{u}_{A_3}$	$\mathbf{u}_{B_3}$	$\mathbf{u}_{A_2}$	$\mathbf{u}_{B_2}$
	$[\mu m]$			
Displacements under force housing deformation				
x	-0.212	1.226	0.020	1.711
y	-0.221	-0.071	-0.203	-0.116
z	-0.720	-1.585	-0.659	-1.595
Displacements under force bearing elastic deformation				
x	0.850	7.104	1.806	4.799
y	-1.142	-7.656	1.787	5.223
z	0.000	0.560	0.000	-0.103
Displacements under temperature housing deformation				
x	-20.659	-29.729	42.06	41.801
y	38.611	76.688	41.422	46.925
z	0.000	0.000	0.000	0.000
Total displacements				
x	-20.021	-21.399	43.886	48.311
y	37.248	68.962	43.006	52.032
z	-0.720	-2.145	-0.659	-1.698

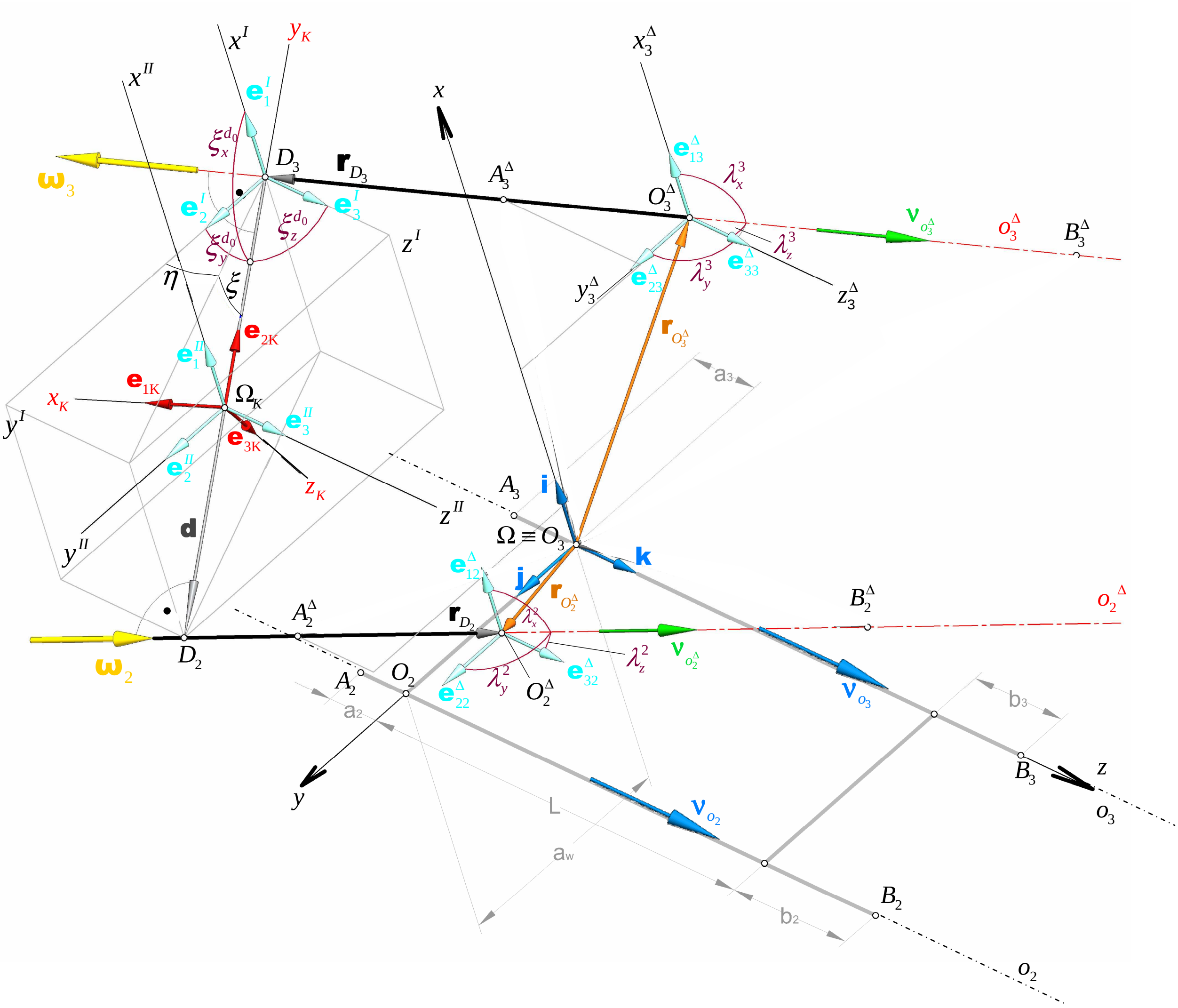

Fig. 10: Axes of rotors in deformed positions with Plücker conoid

where $\mathbf{d} = d\,\mathbf{d}_0$ and unit vector $\mathbf{d}_0 = \dfrac{\mathbf{v}_{o_3^\Delta} \times \mathbf{v}_{o_2^\Delta}}{\left|\mathbf{v}_{o_3^\Delta} \times \mathbf{v}_{o_2^\Delta}\right|}$. The location of the Plücker coordinate system has to fulfilled the condition that transversal d lies on the axis y_k and the origin Ω_k of the coordinate system R_k is at half of the length of the transversal d and angles between the coordinate axis x_k and axes o_{32}^Δ is defined with the equation (5) where $\vartheta = \vartheta_{32}^\Delta = \vartheta_2^\Delta + \gamma_2$ and $tg\,\gamma_2$ is determined with the second equation of the system (1). The position of the axis o_{32}^Δ in the fundamental coordinate system R_k is defined with expressions

$$ {}_{R_k}\mathbf{r}_{o_{32}^\Delta} = \left[0,\ y_{o_{32}^\Delta},\ 0\right]^T , \qquad {}_{R_k}\mathbf{v}_{o_{32}^\Delta} = \left[\cos\vartheta_{32},\ 0,\ \sin\vartheta_{32}\right]^T . \tag{14} $$

For the expression of the axis o_{32}^Δ in the basic coordinate space $R \equiv (\mathbf{i}, \mathbf{j}, \mathbf{k})$ the transformation relation $T : R_k \rightarrow R$ which is given with

$$ {}_R\mathbf{r}_{o_{32}^\Delta} = \mathbf{T}_{R_k R} \cdot {}_{R_k}\mathbf{r}_{o_{32}^\Delta} , \tag{15} $$

to be used. The transformation matrix is given with six sub-matrixes. For transformation of the unit vector $\mathbf{v}_{o_{32}^{\Delta}}$ the using of the rotary matrix $\mathbf{S}_{R_k R}$ that creates the sub-matrix of the matrix $\mathbf{T}_{R_k R}$ is sufficient. Position vectors $_R\mathbf{r}_{o_i^{\Delta}}$ of points O_i^{Δ}, Fig. 10, with unit vectors $_R\mathbf{v}_{o_i^{\Delta}}$, $i = 2, 3$ and the point $_RO_{ij}^{\Delta}$ with the unit vector $_R\mathbf{v}_{o_{ij}^{\Delta}}$, $i = 3,\ j = 2$, Fig. 11, are expressed with their components in Tab. 3. Axes displacement from parallel positions into skew arrangement causes a change in the contact of surfaces. The origin curve contact passes into the point contact. As a result of this mutation the force, transmitted between both rotors, take place at the contact point and not at the curve.

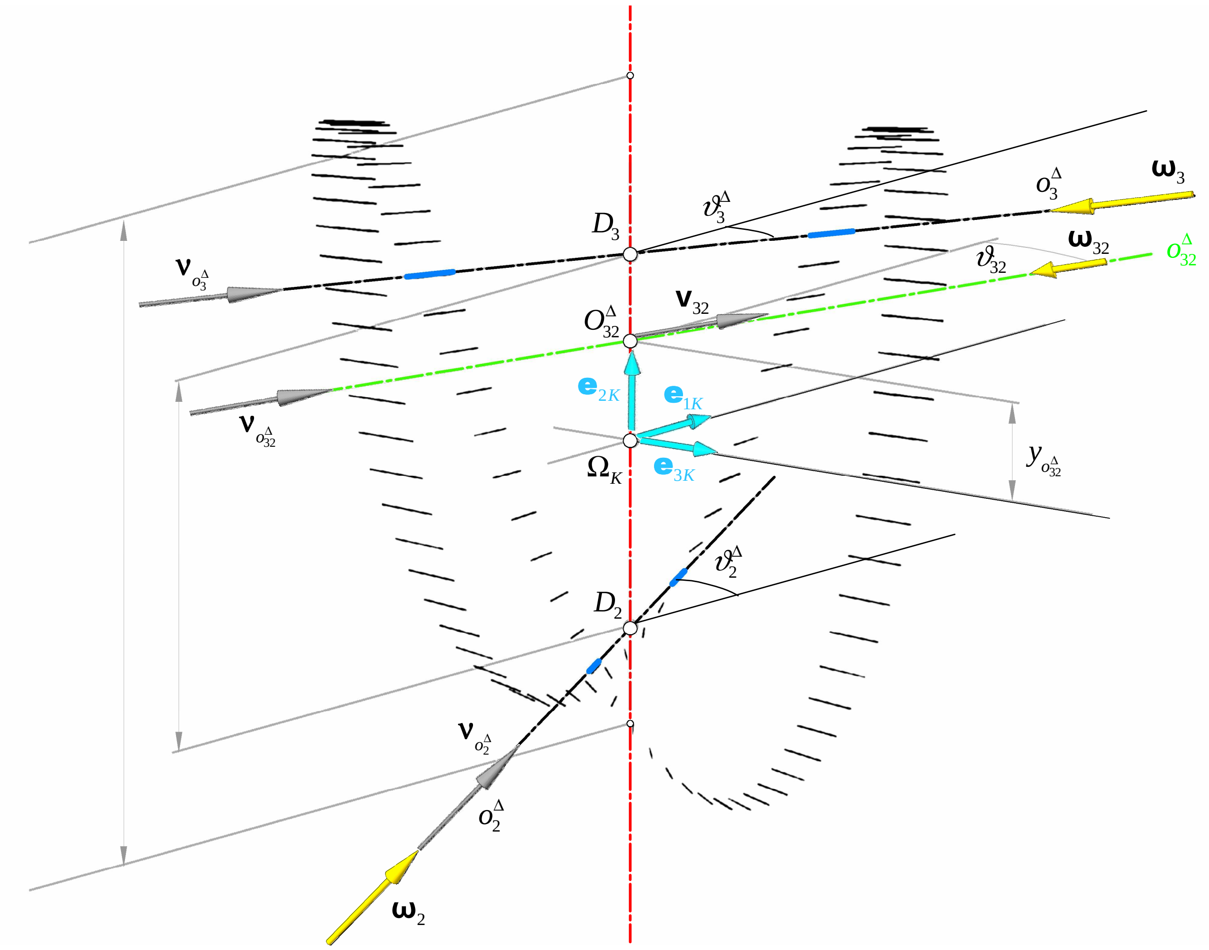

Fig. 11: Position of rotor axes on Plücker conoid

Tab. 3: Components of position vectors and unit vectors of rotor axes

components	$\mathbf{r}_{o_3^{\Delta}}$ [mm]	$\mathbf{v}_{o_3^{\Delta}}$	$\mathbf{r}_{o_2^{\Delta}}$ [mm]	$\mathbf{v}_{o_2^{\Delta}}$	$\mathbf{r}_{o_{32}^{\Delta}}$ [mm]	$\mathbf{v}_{o_{32}^{\Delta}}$
x	0.0015062	0.00002894	0.0022079	0.00001736	2.2043258	0.00002368
y	-0.00208813	-0.00002394	85.0018713	0.00001306	39.3252740	0.00000712
z	-0.0007200	0.99999999	0.0006590	0.99999999	0.0	0,99999999

For the solution of force effects acting on rotors, which have axes in the skew position, in chambers of a work space we use parallel arrangement of rotor axes because the seating displacement of rotors has great influence over the contact of surfaces but little influence upon forces originate in the work space. Reaction forces at points of rotor seating and at the contact point of tooth surfaces we determine by using of the virtual work applied to wrenches and twists. In places of rotor seating and in the contact point of surfaces, Fig. 12, wrenches $\rho_i^m = -\rho_i^{Rm}$, $i = 1 \div 6$, $m = 2, 3$, for simplifying of record the expression ρ_i^m will be

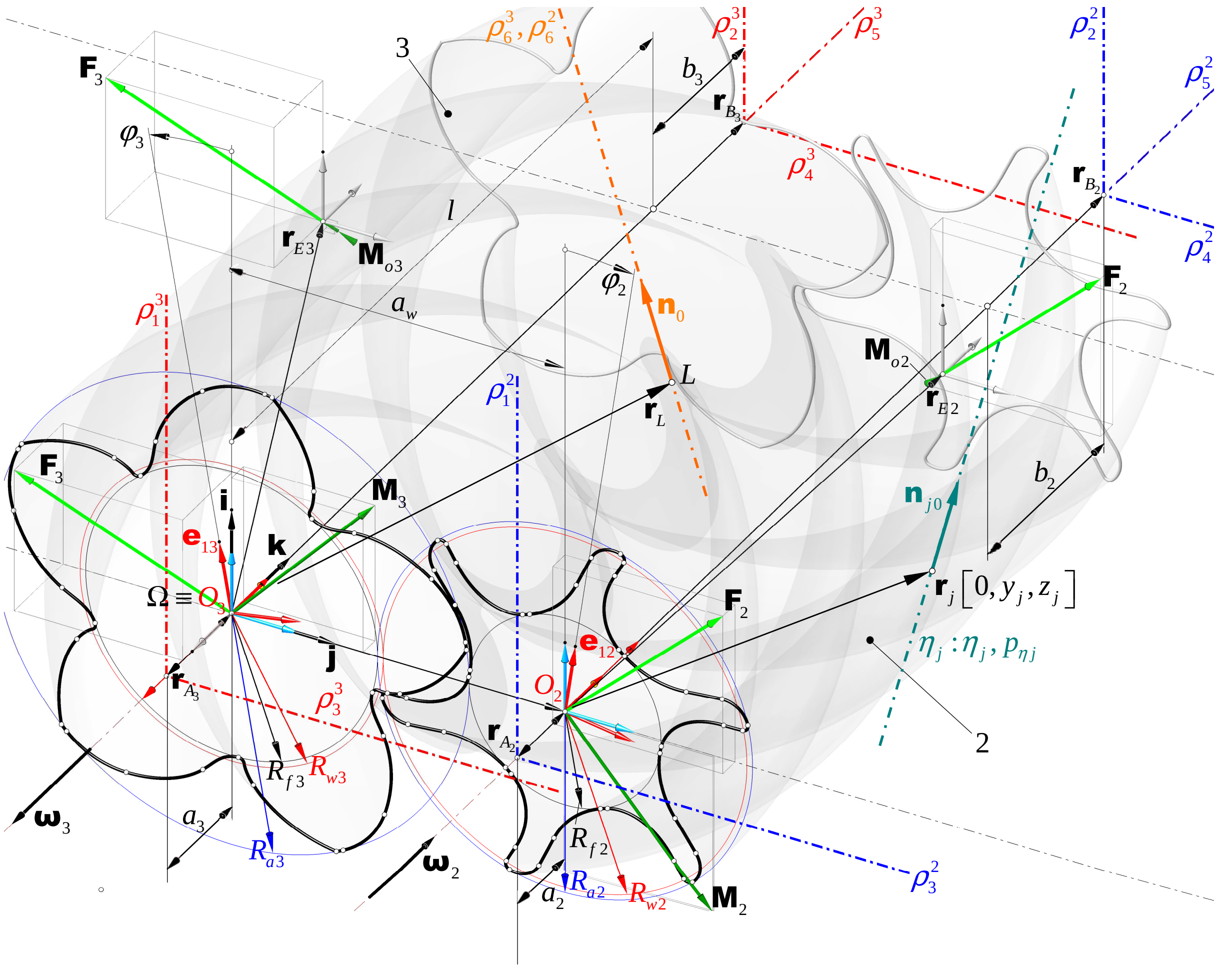

Fig. 12: Wrenches effect on rotors

used, are introduced. Likewise an auxiliary system of twists η_j, $j = 1 \div 6$, was introduced. Using of the equation (11) to all wrenches ρ_i^m we obtain a system of six equations for forces $\rho_i''^m$ for each of rotors. Form one of these equations for twist η_1 is followed

$$\rho_m'' \eta_1' \tilde{\omega}_{\rho_m \eta_1} = \rho_1''^m \eta_1' \tilde{\omega}_{\rho_i^m \eta_1} + \rho_2''^m \eta_1' \tilde{\omega}_{\rho_2^m \eta_1} + \rho_3''^m \eta_1' \tilde{\omega}_{\rho_3^m \eta_1} + \ldots + \rho_6''^m \eta_1' \tilde{\omega}_{\rho_6^m \eta_1} \qquad (16)$$

Other equations for η_j, $j = 2 \div 6$, are similar. The solution was made for four time levels which agree with the angular displacement of the male rotor $\varphi_3 = 0^\circ, 18^\circ, 36^\circ, 54^\circ$. Acting wrenches are shown in the table 1 for the first time level. Position vector of the contact point was determined numerically and its coordinates with the unit vector of the normal in this point are presented in Tab. 4 for the first time level. The system (16) was used for the solution

Tab. 4: Point of contact, unit vector of normal for $\varphi_3 = 0^\circ$

	Point of contact [m]	**Unit vector of normal**
x	0.0130	-0.6107
y	0.0491	-0.4856
z	0.1220	-0.6255

of the female rotor equilibrium, $m = 2$, where the normal force was determined. For the solution of the male rotor equilibrium, $m = 3$, the equation (16) was rewritten, see the equation (11), into form

$$\rho_3'' \tilde{\omega}_{\rho_3 \eta_j} = \rho_1''^3 \tilde{\omega}_{\rho_1^3 \eta_j} + \rho_2''^3 \tilde{\omega}_{\rho_2^3 \eta_j} + ... + \chi \cos\phi_{\rho_5^3 \eta_j} + \rho_5''^3 \left(p_{\eta_j} \cos\phi_{\rho_5^3 \eta_j} - d \sin\phi_{\rho_5^3 \eta_j} + \rho_5''^3 \; \tilde{\omega}_{\rho_6^3 \eta_j} \right) \tag{17}$$

Tab. 5: Reaction effects at bindings of rotors for $\varphi_3 = 0^\circ$

Female rotor					
$\rho_1''^2 [N]$	$\rho_2''^2 [N]$	$\rho_3''^2 [N]$	$\rho_4''^2 [N]$	$\rho_5''^2 [N]$	$\rho_6''^2 [N]$
1288.94	515.83	48.63	797.33	4504.75	6700.61
Male rotor					
$\rho_1''^3 [N]$	$\rho_2''^3 [N]$	$\rho_3''^3 [N]$	$\rho_3''^4 [N]$	$\rho_5''^3 [N]$	$p_{\rho_5^3} [m]$
-2630.76	-3509.78	-1265.09	397.57	-2933.82	-0.037

where $j = 1 \div 6$ and $\chi = \rho_5''^3 \, p_{\rho_5^3}$ is the moment of the couple around the axis z and $\rho_6''^3 = \rho_6''^2$ is the normal force in the point of the contact. Obtained results of reaction effects from numerical solution of both rotors are presented in Tab. 5 for the first time level. A ratio of values of normal forces at the general point of the contact curve and at separated point is 1 : 4915 for the considered distance 0,1 mm between neighbouring bodies of the contact curve on condition uniformly distribute of forces along this curve.

5. Conclusions

Using the theory of screw the relative motion of two rigid bodies with skew axes was solved. The axis of the relative screw motion as well as axes of rotary motions of bodies lying on the Plücker conoid. This theory was applied to toothed rotors of screw machines i.e. screw compressors and screw engines. Already a small displacement of, originally parallel, rotor axes which causes their skew position, leads to a change of the character of the surfaces contact. The original curvilinear contact modified into the point contact. Forces, acting at places of rotor seating and at the contact point of tooth surfaces of rotors, was determined by the help of the theory of screw as well. The change of the contact character causes a significant increasing of the value of the normal force acting between both surfaces. Theory of screws is a suitable instrument for solution of spatial problems of mechanisms with the higher kinematics pairs.

Acknowledgement

This work was supported by the project MSM 4977751303 of the Ministry of Education of the Czech Republic.

References

Altman, F.G. (1937) Bestimmung des Zahnflankeneingriffs bei allgemeinen Schraubgetrieben. *Forschung auf dem Gebiete des Ingenieurwesen Nr. 5*, Berlin, pp. 209-225.

Angeles, J., Figliolini, G., Stachel, H. (2006) On Martin Disteli´s Main Achievements in Spatial Gearing: Disteli´s Diagram. *EuCoMeS – 1st European Conference on Mechanism Science, February 21-26, Obergurgl, Tyrol.*

Ball, R.S. (1998) *A Treatise on the Theory of Screws.* Cambridge University Press, Cambridge. First published 1900.

Bär, G. (2000) *Zur Optimierung der Grundgeometrie von Hypoidgetrieben.* Tagung Antriebstechnik / Zahnradgetriebe TU Dresden. IMM, pp. 372-386.

Figliolini, G., Stachel, H., Angeles J. (2007) A new look at the Ball-Disteli diagram and its relevance to spatial gearing. *Mechanism and Machine Theory 42*, pp. 1362-1375.

Kadeřávek, F., Klíma, J., Kounovský, J. (1932) *Descriptive geometry II* (in Czech). Library of mathematical and physical writings, Volume 17, Prague.

Šejvl, M. (1967) *Applied kinematics to spatial gearing* (in Czech). Doctoral thesis, Pilsen.

Švígler, J., Machulda, V., Siegl, J. (2006) Deformation of Screw Machine Housing under Force Field and its Consequences. *VDI Berichte Nr. 1932 Schraubenmaschinen 2006,* Dortmund, pp. 377-388.